Brain Accumulation of Dasatinib Is Restricted by P-Glycoprotein (ABCB1) and Breast Cancer Resistance Protein (ABCG2) and Can Be Enhanced by Elacridar Treatment

Jurjen S. Lagas,[1] Robert A.B. van Waterschoot,[1] Vicky A.C.J. van Tilburg,[1] Michel J. Hillebrand,[2] Nienke Lankheet,[2] Hilde Rosing,[2] Jos H. Beijnen,[2] and Alfred H. Schinkel[1]

Abstract

Purpose: Imatinib, a BCR-ABL tyrosine kinase inhibitor, is a substrate of the efflux transporters P-glycoprotein (P-gp; *ABCB1*) and ABCG2 (breast cancer resistance protein), and its brain accumulation is restricted by both transporters. For dasatinib, an inhibitor of SCR/BCR-ABL kinases, *in vivo* interactions with P-gp and ABCG2 are not fully established yet.

Experimental Design: We used *Abcb1a/1b*$^{-/-}$, *Abcg2*$^{-/-}$, and *Abcb1a/1b;Abcg2*$^{-/-}$ mice to establish the roles of P-gp and ABCG2 in the pharmacokinetics and brain accumulation of dasatinib.

Results: We found that oral uptake of dasatinib is limited by P-gp. Furthermore, relative brain accumulation, 6 hours after administration, was not affected by Abcg2 deficiency, but absence of P-gp resulted in a 3.6-fold increase after oral and 4.8-fold higher accumulation after i.p. administration. *Abcb1a/1b;Abcg2*$^{-/-}$ mice had the most pronounced increase in relative brain accumulation, which was 13.2-fold higher after oral and 22.7-fold increased after i.p. administration. Moreover, coadministration to wild-type mice of dasatinib with the dual P-gp and ABCG2 inhibitor elacridar resulted in a similar dasatinib brain accumulation as observed for *Abcb1a/1b;Abcg2*$^{-/-}$ mice.

Conclusions: Brain accumulation of dasatinib is primarily restricted by P-gp, but Abcg2 can partly take over this protective function at the blood-brain barrier. Consequently, when both transporters are absent or inhibited, brain uptake of dasatinib is highly increased. These findings might be clinically relevant for patients with central nervous system Philadelphia chromosome–positive leukemia, as coadministration of an inhibitor of P-gp and ABCG2 with dasatinib might result in better therapeutic responses in these patients.

Multidrug efflux transporters of the ATP-binding cassette (ABC) transporter family, such as P-glycoprotein (P-gp; *ABCB1*), breast cancer resistance protein (*ABCG2*), and multidrug resistance protein 2 (*ABCC2*), can have an important effect on chemotherapy. These efflux pumps have a broad and overlapping substrate specificity and are expressed at apical membranes of important epithelial barriers and at the canalicular membrane of hepatocytes. Consequently, these proteins can facilitate excretion of transported drugs via liver, intestine, and kidneys and restrict the intestinal uptake of orally encountered substrates. In addition, ABC transporters are localized at the so-called sanctuary site barriers, such as blood-brain, blood-testis, and blood-placenta barrier, where they restrict accumulation of potentially harmful compounds. Moreover, (over-)expression of these efflux pumps in tumor cells can lead to multidrug resistance through active efflux of cytostatic drugs (1).

Imatinib, a first-generation, orally active inhibitor of BCR-ABL kinase, is currently used as frontline therapy for Philadelphia chromosome–positive (Ph+) leukemia (defined by the fusion of the *BCR* and *ABL* genes), including chronic myeloid leukemia (CML) and Ph+ acute lymphoblastic leukemia. Imatinib has revolutionized the treatment of CML by its impressive therapeutic responses in the chronic phase of the disease. However, patients with advanced disease show generally lower and more transient responses to imatinib. In addition, accumulating evidence indicates that resistance to imatinib in a significant proportion of patients in all disease stages results in failure to achieve an optimal response (2–4). Thus far, several mechanisms of resistance have been reported, including point mutations in the BCR-ABL kinase domain, amplification of the gene, and imatinib binding to α_1-acid glycoprotein (5–9).

Dasatinib is a second-generation, oral, multitargeted inhibitor of BCR-ABL and SRC family kinases, rationally designed for CML treatment (10). Compared with imatinib, dasatinib has 325-fold

Authors' Affiliations: [1]Division of Molecular Biology, The Netherlands Cancer Institute; [2]Department of Pharmacy and Pharmacology, Slotervaart Hospital, Amsterdam, the Netherlands

Received 8/29/08; revised 12/22/08; accepted 12/29/08; published OnlineFirst 3/10/09.

Grant support: Dutch Cancer Society grants NKI-2003-2940 and 2007-3764 and Technical Sciences Foundation of the Netherlands Organization for Scientific Research grant BFA.6165.

The costs of publication of this article were defrayed in part by the payment of page charges. This article must therefore be hereby marked *advertisement* in accordance with 18 U.S.C. Section 1734 solely to indicate this fact.

Requests for reprints: Alfred H. Schinkel, Division of Molecular Biology, The Netherlands Cancer Institute, Plesmanlaan 121, 1066 CX Amsterdam, the Netherlands. Phone: 31-20-5122046; Fax: 31-20-6691383; E-mail: a.schinkel@nki.nl.

doi:10.1158/1078-0432.CCR-08-2253

Translational Relevance

A significant proportion of chronic myeloid leukemia and Philadelphia chromosome – positive (Ph+) acute lymphoblastic leukemia patients treated with imatinib develops central nervous system (CNS) relapses. Recently, for the second-generation tyrosine kinase inhibitor dasatinib, substantial antitumor activity was shown in a mouse model of intracranial Ph+ leukemia, whereas imatinib had no effect. In the same study, dasatinib showed substantial activity in 11 patients with CNS Ph+ leukemia. Although these results are impressive, brain accumulation of dasatinib is still relatively low.

We show that mice deficient for the drug efflux transporters P-glycoprotein (P-gp) and ABCG2 have drastically increased dasatinib brain concentrations, both after oral and i.p. administration. Moreover, we show that the dual P-gp and ABCG2 inhibitor elacridar can substantially increase dasatinib brain accumulation in wild-type mice. Our findings provide a rationale for combining dasatinib with a dual P-gp and ABCG2 inhibitor to improve the therapeutic efficacy of dasatinib in patients with CNS Ph+ leukemia.

greater *in vitro* potency against cells expressing "wild-type" (WT) BCR-ABL (11). Furthermore, dasatinib effectively inhibits the growth of clones of a leukemic cell line expressing all known imatinib-resistant BCR-ABL isoforms, with the exception of T315I (12). Importantly, dasatinib has shown significant activity in imatinib-resistant or imatinib-intolerant patients with CML or Ph+ acute lymphoblastic leukemia (13 – 17).

Imatinib is a substrate of the efflux transporters P-gp and ABCG2 and penetration of imatinib through the blood-brain barrier is markedly restricted by both transporters (18 – 27). This might explain why up to 20% of the imatinib-treated patients with either lymphoid or myeloid blast crisis CML or Ph+ acute lymphoblastic leukemia develop central nervous system (CNS) relapses (28, 29). In contrast, dasatinib was recently found to have antitumor activity in a mouse model of intracranial CML, and in patients with CNS Ph+ leukemia, dasatinib induced substantial responses (30). Moreover, in K562 leukemic cells that overexpress P-gp, dasatinib showed significant antiproliferation activity, in contrast to imatinib (31). These findings may indicate that dasatinib is not seriously affected by P-gp and/or ABCG2 at the blood-brain barrier or by P-gp in the K562 cells. Nonetheless, it was recently found that the accumulation of dasatinib was decreased in P-gp – overexpressing and ABCG2-overexpressing leukemic cells and that dasatinib was transported in P-gp – overexpressing MDCK-II cells, suggesting that dasatinib is a substrate of P-gp and ABCG2 (32, 33).

To further study the interaction of dasatinib with drug transporters, we used *in vitro* Transwell transport assays. In addition, *Abcb1a/1b*$^{-/-}$, *Abcg2*$^{-/-}$, and *Abcb1a/1b;Abcg2*$^{-/-}$ mice were used to investigate the *in vivo* roles of P-gp and ABCG2 in the pharmacokinetics and brain accumulation of dasatinib.

Materials and Methods

Chemicals. Dasatinib monohydrate originated from Sequoia Research Products. GlaxoSmithKline kindly provided Elacridar (GF120918). [^{14}C]Inulin was from Amersham. Methoxyflurane (Metofane) was from Medical Developments Australia. Bovine serum albumin, fraction V, was from Roche. All other chemicals and reagents were obtained from Sigma-Aldrich.

Transport assays. Polarized canine kidney MDCK-II cell lines were used in transport assays. MDCK-II cells transduced with human ABCB1 or ABCC2 or murine Abcg2 were described previously (34, 35). Transepithelial transport assays using Transwell plates were carried out as described previously with minor modifications (36). Experiments with cells transfected with human ABCC2 were done in the presence of 5 μmol/L elacridar to inhibit any endogenous P-gp activity. Elacridar does not affect ABCC2 activity. When elacridar was applied, it was present in both compartments during 2-h preincubation and during the transport experiment. After preincubation, experiments were started (t = 0) by replacing the medium in either the apical or basolateral compartment with fresh Opti-MEM medium (Invitrogen), either with or without 5 μmol/L elacridar and containing 5 μmol/L of dasatinib. Cells were incubated at 37°C in 5% CO_2, and 50 μL aliquots were taken at t = 2 and 4 h. Transport was calculated as the fraction of drug found in the acceptor compartment relative to the total amount added to the donor compartment at the beginning of the experiment. Transport is given as mean percentage ± SD (n = 3). Membrane tightness was assessed in parallel, using the same cells seeded on the same day and at the same density, by analyzing transepithelial [^{14}C]inulin (~3 kBq/well) leakage. Leakage had to remain <1% of the total added radioactivity per hour.

Relative transport ratio. Active transport was expressed by the relative transport ratio (r), defined as r = percentage apically directed transport divided by percentage basolaterally directed translocation, after 4 h (37).

Animals. Mice were housed and handled according to institutional guidelines complying with Dutch legislation. Animals used were male WT, *Abcb1a/1b*$^{-/-}$ (38), *Abcg2*$^{-/-}$ (35), and *Abcb1a/1b;Abcg2*$^{-/-}$ (39) mice, all of a >99% FVB genetic background, between 10 and 12 wk of age. Animals were kept in a temperature-controlled environment with a 12-h light/12-h dark cycle and received a standard diet (AM-II, Hope Farms) and acidified water *ad libitum*.

Plasma pharmacokinetics. Dasatinib was dissolved in DMSO (25 mg/mL) and 25-fold diluted with 50 mmol/L sodium acetate buffer (pH 4.6). For oral studies, dasatinib was dosed at 10 mg/kg body weight (10 mL/kg). To minimize variation in absorption, mice were fasted 3 h before dasatinib was administered by gavage into the stomach using a blunt-ended needle. For plasma pharmacokinetic studies after systemic exposure, dasatinib was applied by i.p. injection because i.v. injection into a tail vein compromises multiple blood sampling from the tail. For i.p. studies, dasatinib was dosed at 5 mg/kg body weight (5 mL/kg). We used a 2-fold lower dose for i.p. than for oral studies to obtain plasma concentrations and area under plasma concentration-time curve (AUC) values that are in the same range for both administration routes. Multiple blood samples (~50 μL) were collected from the tail vein at 7.5 min (i.p.) or 15 min (oral) and 30 min and 1, 2, 4, and 6 h (both series) using heparinized capillary tubes (Oxford Labware). At the last time point, mice were anesthetized with methoxyflurane and blood was drawn by cardiac puncture. Immediately thereafter, mice were sacrificed by cervical dislocation and brains were rapidly removed, homogenized on ice in 4% bovine serum albumin, and stored at -20°C until analysis. Blood samples were centrifuged at 2,100 × g for 6 min at 4°C, and the plasma fraction was collected, completed to 200 μL with drug-free human plasma, and stored at -20°C until analysis.

Brain accumulation of dasatinib in combination with elacridar. Elacridar was dissolved in a mixture of ethanol, polyethylene glycol 200, and 5% glucose (2:6:2) and i.v. injected into a tail vein at 10 mg/kg (2.5 mL/kg). Dasatinib dissolved in DMSO (25 mg/mL) was 25-fold diluted with 50 mmol/L sodium acetate buffer (pH 4.6) and injected as a single i.v. bolus at 5 mg/kg body weight (5 mL/kg). Dasatinib was administered 15 min after an injection with either

elacridar or with the vehicle used to dissolve elacridar. Blood and brains were isolated 60 min after dasatinib administration and processed and stored as described above.

Relative brain accumulation. Brain concentrations were corrected for the amounts of drug in the brain vasculature (i.e., 1.4% of the plasma concentration right before the brains were isolated; ref. 22). Subsequently, brain accumulation after oral or i.p. dasatinib administration was calculated by determining the dasatinib brain concentration relative to the AUC from 0 to 6 h ($AUC_{0\text{-}6}$). For studies with i.v. dasatinib in combination with elacridar, blood was collected only just before the brains were isolated, 60 min after dasatinib administration. Therefore, brain-to-plasma ratios were calculated to assess the relative brain accumulation.

Drug analysis. Dasatinib concentrations in Opti-MEM cell culture medium and in plasma samples and brain homogenates were determined using a sensitive and specific liquid chromatography-tandem mass spectrometry (LC-MS/MS) assay. Chromatography was carried out using a Solvent delivery system LC-20AD Prominence (Shimadzu), consisting of a binary pump, autosampler, degasser, and column oven. Chromatographic separations of the analytes were carried out on a Gemini C18 column, 50 × 2.0 mm internal diameter, 5 μm (Phenomenex). A mobile phase consisting of eluent A (10 mmol/L ammonium hydroxide in water) and eluent B (1 mmol/L ammonium hydroxide in methanol) was pumped through the column with a flow of 0.25 mL/min. The following gradient was used:

Time (min)	0.0	0.5	3.0	6.0	6.1	8.0	8.1	12.0
Eluent B (%)	55	55	80	80	100	100	55	55

The respective retention time for dasatinib was 3.8 min. The mass spectrometric analyses were done using a Finnigan TSQ Quantum Ultra Triple Quadrupole Spectrometer equipped with an electrospray ion source (Thermo Fisher). The mass spectrometers were operating in positive electrospray selective multiple reaction monitoring, and three multiple reaction monitoring channels were monitored at unit resolution corresponding to dasatinib *m/z* 488 to 401, and the stable ^{13}C isotope of imatinib *m/z* 498 to 394 (used as internal standard). Samples were pretreated by protein precipitation with acetonitrile, and the supernatants were diluted 1:1, v/v (sample extract: eluent A) before injection (10 μL).

Pharmacokinetic calculations and statistical analysis. Pharmacokinetic parameters were calculated by noncompartmental methods using the software package WinNonlin Professional version 5.0. The AUC was calculated using the trapezoidal rule, without extrapolating to infinity. Elimination half-lives ($t_{1/2,\ el}$) were calculated by linear regression analysis of the log-linear part of the plasma concentration-time curves. The peak plasma concentration (C_{max}) and the time of maximum plasma concentration (T_{max}) were estimated from the original data. Apparent clearance (CL_{app} or CL/F) was calculated by the formula CL_{app} = dose/AUC. The relative oral bioavailability (F_{rel}) was calculated by the formula $F_{rel} = (AUC_{oral} \times Dose_{i.p.})/(AUC_{i.p.} \times Dose_{oral}) \times 100\%$. The two-sided unpaired Student's *t* test was used for statistical analysis. Data obtained with single and combination knockout (KO) mice were compared with data obtained with WT mice. Differences were considered statistically significant when $P < 0.05$. Data are presented as means ± SD.

Results

In vitro *transport of dasatinib.* We used monolayers of the polarized canine kidney cell line MDCK-II and its subclones transduced with human ABCB1 or ABCC2 or murine Abcg2 to study transepithelial vectorial transport of 5 μmol/L dasatinib. Dasatinib was modestly but actively transported in the apical direction in the MDCK-II parental cell line (Fig. 1A), which is known to have relatively high expression of functional endogenous canine P-gp (40). Transport in the parental cells could be completely inhibited with elacridar, a potent inhibitor of P-gp (Fig. 1D), suggesting that indeed endogenous P-gp was responsible for dasatinib transport in the parental cells. In cells transfected with murine Abcg2 or human ABCB1 P-gp, transport of dasatinib was markedly increased, resulting in

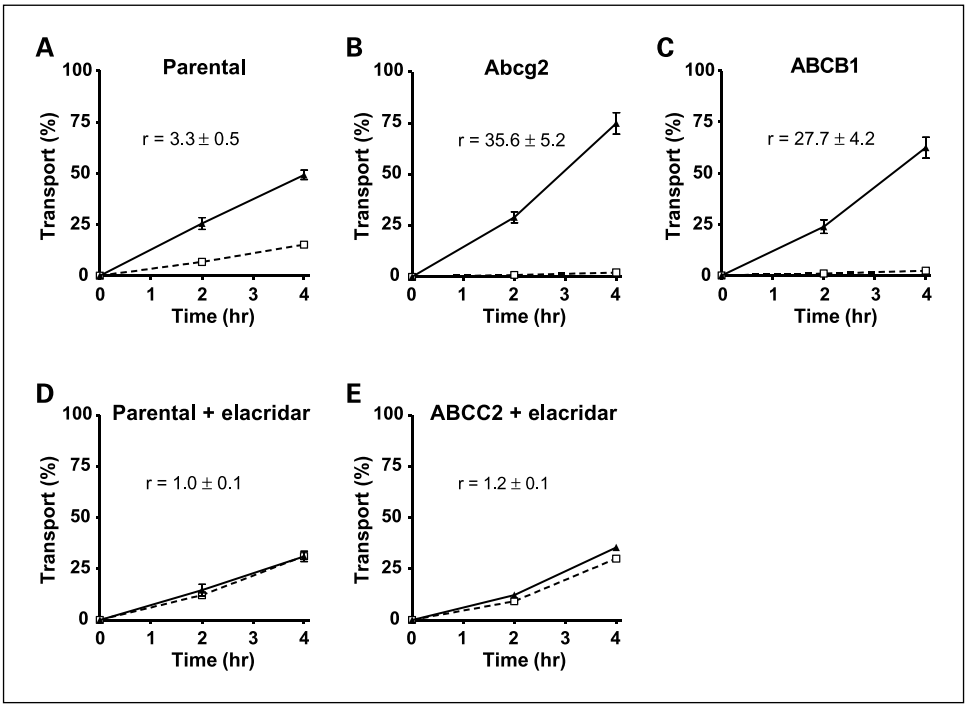

Fig. 1. Transepithelial transport of dasatinib (5 μmol/L) was assessed in MDCK-II cells either nontransduced (*A* and *D*) or transduced with murine Abcg2 (*B*) or human ABCB1 (*C*) or ABCC2 (*E*) cDNA. At $t = 0$ h, dasatinib was applied in one compartment (apical or basolateral), and the concentration in the opposite compartment at $t = 2$ and 4 h was measured by LC-MS/MS and plotted as the percentage of initial drug concentration ($n = 3$). *D* and *E*, elacridar (5 μmol/L) was applied to inhibit endogenous P-gp. ▲, translocation from the basolateral to the apical compartment; □, translocation from the apical to the basolateral compartment. Points, mean; bars, SD. At $t = 4$ h, 1% of transport is approximately equal to an apparent permeability coefficient (P_{app}) of 0.30×10^{-6} cm/s.

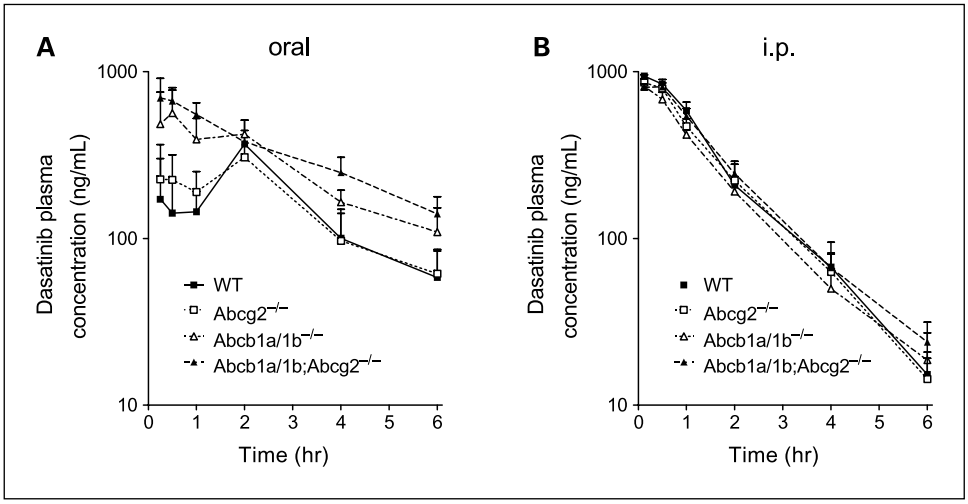

Fig. 2. Plasma concentration-time curves of dasatinib in male FVB WT (■), *Abcg2*$^{-/-}$ (□), *Abcb1a/1b*$^{-/-}$ (Δ), and *Abcb1a/1b;Abcg2*$^{-/-}$ (▲) mice after oral (*A*) and i.p. (*B*) administration of dasatinib at a dose of 10 mg/kg (oral) and 5 mg/kg (i.p.). Points, mean (n = 5 for oral and n = 4 for i.p. administration); bars, SD.

10.8- and 8.4-fold higher transport ratios (r, defined in Materials and Methods) compared with parental cells, respectively (Fig. 1B and C). In cells transduced with human ABCC2, no transport of dasatinib was observed (Fig. 1E).

Effect of ABCG2 and P-gp on plasma pharmacokinetics of dasatinib in mice. Because our data indicated that both ABCG2 and P-gp have a profound effect on dasatinib transport *in vitro*, we further investigated their separate and combined effect *in vivo*. In the clinic, dasatinib is administered orally to cancer patients, and therefore, we first studied plasma dasatinib concentrations after oral administration of 10 mg/kg to WT, *Abcb1a/1b*$^{-/-}$, *Abcg2*$^{-/-}$, and *Abcb1a/1b;Abcg2*$^{-/-}$ mice. *Abcb1a/1b*$^{-/-}$ mice displayed a 1.7-fold higher AUC_{oral} compared with WT mice (P < 0.05; Fig. 2A; Table 1), and the maximal plasma levels in *Abcb1a/1b*$^{-/-}$ mice were reached markedly faster than in WT mice. In WT mice, the relatively late C_{max}, ~2 hours after oral administration, might partly be explained by enterohepatic circulation of dasatinib. The fact that this late C_{max} was absent in P-gp–deficient animals may indicate that P-gp restricts rapid absorption from the intestine and/or mediates substantial hepatobiliary excretion and thus contributes to enterohepatic circulation of dasatinib. Deficiency of only Abcg2 did not affect plasma pharmacokinetics after oral administration (Fig. 2A; Table 1). *Abcb1a/1b;Abcg2*$^{-/-}$ mice had 2.0-fold higher AUC_{oral} (P < 0.01), and the C_{max} was 1.9-fold higher compared with WT mice (P < 0.05; Fig. 2A; Table 1). Collectively, these results indicate that P-gp, and not Abcg2, restricts the oral uptake of dasatinib in mice.

To study the plasma pharmacokinetics after systemic administration, dasatinib was given by i.p. injection at 5 mg/kg. At this dose, plasma concentrations were in the same range as in oral experiments with 10 mg/kg. *Abcb1a/1b*$^{-/-}$ mice had slightly, but significantly, lower plasma concentrations 0.5 and 1 hour after administration, resulting in a 1.3-fold lower $AUC_{i.p.}$ compared with WT mice (P < 0.05; Fig. 2B; Table 1). The $AUC_{i.p.}$ values for *Abcg2*$^{-/-}$ and *Abcb1a/1b;Abcg2*$^{-/-}$ mice were not

Table 1. Plasma pharmacokinetic parameters after oral (10 mg/kg) or i.p. (5 mg/kg) administration of dasatinib

	Strain			
	WT	***Abcb1a/1b*$^{-/-}$**	***Abcg2*$^{-/-}$**	***Abcb1a/1b;Abcg2*$^{-/-}$**
Oral				
$AUC_{(0-6)}$ (mg/L.h)	1.02 ± 0.27	1.70 ± 0.42*	1.00 ± 0.35	2.05 ± 0.25 †
C_{max} (mg/L)	0.37 ± 0.08	0.49 ± 0.27	0.31 ± 0.21	0.70 ± 0.22*
T_{max} (h)	2	0.5	2	0.25
CL_{app} (L/h.kg)	10.4 ± 2.40	6.15 ± 1.38 †	11.0 ± 3.61	4.94 ± 0.58 †
I.p.				
$AUC_{(0-6)}$ (mg/L.h)	1.59 ± 0.10	1.25 ± 0.15*	1.69 ± 0.32	1.52 ± 0.16
C_{max} (mg/L)	0.94 ± 0.07	0.81 ± 0.06	0.86 ± 0.07	0.81 ± 0.03*
$t_{1/2,\ el}$ (h)	0.93 ± 0.04	1.43 ± 0.49	0.98 ± 0.28	1.33 ± 0.12*
CL_{app} (L/h.kg)	3.16 ± 0.20	4.05 ± 0.50*	3.05 ± 0.66	3.31 ± 0.36
F_{rel} (%)	32.0 ± 1.74	68.0 ± 3.72 †	29.6 ± 2.39	67.3 ± 2.13 †

NOTE: Data are means ± SD, n = 5 for oral and n = 4 for i.p. administration. All parameters obtained for KO mice were compared with those for WT mice.
Abbreviations: C_{max}, maximum plasma levels; $t_{1/2,\ el}$, elimination half-life, calculated from 2 to 6 h; CL_{app}, apparent clearance (CL/F); F_{rel}, relative oral bioavailability.
*P < 0.05, compared with WT mice.
†P < 0.01, compared with WT mice.

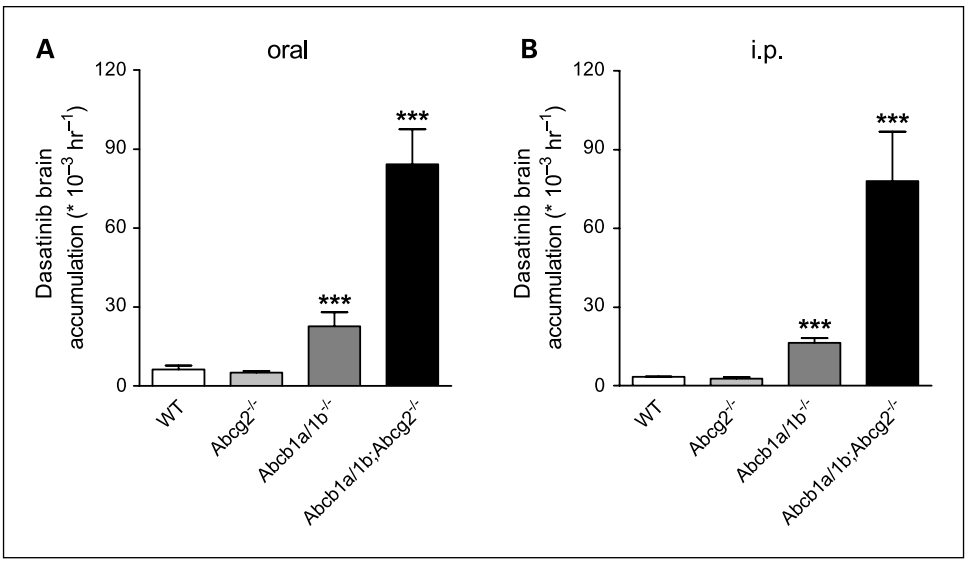

Fig. 3. Relative brain accumulation of dasatinib in male FVB WT, *Abcg2*$^{-/-}$, *Abcb1a/1b*$^{-/-}$, and *Abcb1a/1b;Abcg2*$^{-/-}$ mice after oral (*A*) or i.p. (*B*) administration of dasatinib at a dose of 10 mg/kg (oral) or 5 mg/kg (i.p.). Relative brain accumulation was calculated by determining the brain concentration relative to AUC_{0-6}. Columns, mean (n = 5 for oral and n = 4 for i.p. administration); bars, SD. ***, $P < 0.001$, compared with WT mice.

different from WT mice. These results indicate that both transporters do not strongly affect the systemic distribution and elimination of dasatinib. Because we do not know if the availability after i.p. administration is complete, we used the $AUC_{i.p.}$ as a relative standard to calculate the relative oral bioavailability (F_{rel}) in the different mouse strains. WT and *Abcg2*$^{-/-}$ mice displayed a relative oral bioavailability of ~30% and P-gp deficiency increased the relative oral availability in both *Abcb1a/1b*$^{-/-}$ and *Abcb1a/1b;Abcg2*$^{-/-}$ mice to ~68% ($P < 0.01$; Table 1).

Effect of ABCG2 and P-gp on brain accumulation of dasatinib in mice. As shown in Fig. 3, the relative brain accumulation, determined 6 hours after administration and corrected for the plasma AUC_{0-6}, was not different between *Abcg2*$^{-/-}$ and WT mice, either after oral (Fig. 3A) or i.p. (Fig. 3B) administration. However, in *Abcb1a/1b*$^{-/-}$ mice, the relative brain accumulation was 3.6-fold increased after oral and 4.8-fold higher after i.p. administration. *Abcb1a/1b;Abcg2*$^{-/-}$ mice had the most pronounced increases in relative brain accumulation, 13.2-fold after oral and 22.7-fold after i.p. administration. The relative brain accumulation values as well as the uncorrected brain concentrations are listed in Table 2. Correction for plasma concentration at t = 6 hours yielded qualitatively the same results for relative brain accumulation as correction for AUC_{0-6} (data not shown). These results show that P-gp almost completely controls the dasatinib brain accumulation no matter whether Abcg2 is present or not. However, in *Abcb1a/1b*$^{-/-}$ mice, Abcg2 can partly but not completely take over the function of P-gp at the blood-brain barrier. These results further show that when both transporters are absent, brain accumulation of dasatinib is highly increased.

Effect of the dual P-gp and ABCG2 inhibitor elacridar on dasatinib brain accumulation. Because both P-gp and ABCG2 markedly restricted the brain accumulation of dasatinib, we investigated if inhibition of both efflux transporters at the blood-brain barrier would result in an increased brain accumulation of dasatinib. We used the dual P-gp and ABCG2 inhibitor elacridar. Figure 4A shows that the dasatinib plasma concentration, 60 minutes after i.v. administration, was 1.7-fold higher in *Abcb1a/1b;Abcg2*$^{-/-}$ compared with WT mice ($P < 0.05$). In the presence of elacridar, plasma concentrations of dasatinib in WT and *Abcb1a/1b;Abcg2*$^{-/-}$ mice were not different anymore, suggesting that elacridar inhibits the systemic elimination of dasatinib via P-gp and/or Abcg2. In

Table 2. Brain concentrations and relative brain accumulation after oral (10 mg/kg) or i.p. (5 mg/kg) administration of dasatinib

	Strain			
	WT	***Abcb1a/1b*$^{-/-}$**	***Abcg2*$^{-/-}$**	***Abcb1a/1b;Abcg2*$^{-/-}$**
Oral				
C_{brain} (ng/g)	6.50 ± 2.10	37.2 ± 5.38*	4.93 ± 1.13	171.6 ± 30.9*
P_{brain} ($\times 10^{-3}$ h^{-1})	6.39 ± 1.39	22.7 ± 5.41*	5.11 ± 0.68	84.3 ± 13.3*
I.p.				
C_{brain} (ng/g)	5.47 ± 0.38	25.6 ± 3.56*	5.15 ± 1.73	116.7 ± 15.2*
P_{brain} ($\times 10^{-3}$ h^{-1})	3.44 ± 0.17	16.4 ± 1.71*	2.78 ± 0.65	78.1 ± 18.8*

NOTE: Data are means ± SD, n = 5 for oral and n = 4 for i.p. administration. All parameters obtained for KO mice were compared with those for WT mice.
Abbreviations: C_{brain}, brain concentration at 6 h after administration; P_{brain}, relative brain accumulation at 6 h after administration, calculated by determining the dasatinib brain concentration relative to AUC_{0-6}.
*$P < 0.001$, compared with WT mice.

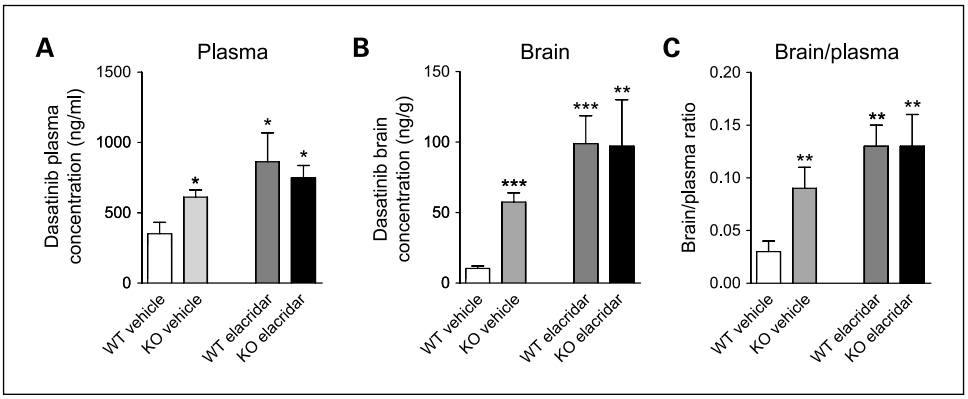

Fig. 4. Plasma (*A*) and brain (*B*) concentrations and brain-to-plasma ratios (*C*) for FVB WT and *Abcb1a/1b;Abcg2*$^{-/-}$ (KO) mice 60 min after i.v. administration of 5 mg/kg dasatinib. Dasatinib was given 15 min after the i.v. administration of either vehicle or elacridar (10 mg/kg). Columns, mean (n = 4 for WT and n = 3 for KO); bars, SD. *, $P < 0.05$; **, $P < 0.01$; ***, $P < 0.001$, compared with WT mice treated with vehicle.

contrast to the modest effect on plasma concentrations, elacridar drastically increased brain concentration in WT mice by 10-fold ($P < 0.001$; Fig. 4B). Brain concentrations in *Abcb1a/1b;Abcg2*$^{-/-}$ mice seemed also somewhat increased when elacridar was applied, but the difference was not statistically significant ($P = 0.11$; Fig. 4B) and probably reflects the modestly higher plasma levels (Fig. 4A). Figure 4C shows the brain-to-plasma ratios, which were calculated to correct for the differences in plasma concentrations. For WT mice, the ratio was 4.4-fold increased with elacridar, resulting in a similar dasatinib brain accumulation as observed for *Abcb1a/1b;Abcg2*$^{-/-}$ mice. For *Abcb1a/1b;Abcg2*$^{-/-}$ mice, elacridar did not affect brain-to-plasma ratios. Overall, these results show that elacridar can completely inhibit P-gp and ABCG2 at the blood-brain barrier, leading to highly increased dasatinib concentrations in the brain.

Discussion

In this study, we show that the second-generation tyrosine kinase inhibitor dasatinib is efficiently transported *in vitro* by P-gp and Abcg2. We extended these observations *in vivo* and found that relative oral availability is limited by P-gp. We further show that the brain accumulation of dasatinib is primarily restricted by P-gp but that Abcg2 can partly take over this protective function at the blood-brain barrier. Consequently, when both efflux transporters are absent, brain uptake of dasatinib is highly increased. And finally, we show that the brain accumulation of dasatinib in WT mice can be markedly increased by applying the dual P-gp and ABCG2 inhibitor elacridar.

It was recently reported that the cellular accumulation of dasatinib in P-gp–overexpressing or ABCG2-overexpressing leukemic cells was significantly lower than in control cells (32). In addition, active transport of dasatinib in P-gp–overexpressing MDCK-II cells was recently shown (33). Our *in vitro* data on the transport of dasatinib by human P-gp are consistent with these observations, and we further show that, in addition to the reported transport by human ABCG2 (32), also mouse Abcg2 is an efficient transporter for dasatinib. Based on the reported *in vitro* data and our own *in vitro* results, we further investigated the effect of P-gp and Abcg2 on the pharmacokinetics of dasatinib. We found that *Abcb1a/1b*$^{-/-}$ mice had 1.7-fold higher plasma AUC_{oral} than WT mice. In a recent study, no difference in AUC_{oral} between WT and P-gp–deficient mice was observed (41). However, the limited number of animals used in that study (n = 3) may have resulted in substantial variation (the variation was not reported). In addition, we know from experience that variation in absorption after oral administration can be markedly reduced by food deprivation for 3 hours before administration. We did so and we used five animals per group, resulting in more statistical power to detect differences in AUC_{oral}.

We found no difference in AUC_{oral} between *Abcg2*$^{-/-}$ and WT mice, despite our observation that dasatinib is a good Abcg2 substrate *in vitro*. Moreover, *Abcb1a/1b;Abcg2*$^{-/-}$ mice had a similar AUC_{oral} compared with *Abcb1a/1b*$^{-/-}$ mice, indicating that P-gp, and not Abcg2, restricts the oral uptake of dasatinib in mice. We have shown earlier that there is not a higher level of P-gp RNA in the intestine of *Abcg2*$^{-/-}$ mice,[3] so possible P-gp up-regulation cannot explain the lack of effect of Abcg2. We further show that the relative oral bioavailability of dasatinib of ~32% in WT mice was more than doubled to ~68% in P-gp–deficient mice. This might be clinically relevant because dasatinib is taken orally by cancer patients, and intestinal uptake in humans might be limited by P-gp as well.

In addition to the effect of P-gp on the relative oral availability, we show that P-gp, together with ABCG2, drastically restricts the brain accumulation of dasatinib in mice. It is interesting to note that P-gp seems to have a dominant role compared with Abcg2 in both intestine and blood-brain barrier, whereas *in vitro* both transporters seem to efficiently transport dasatinib. A possible explanation of this apparent discrepancy could be that Abcg2 is more lowly expressed in intestine and blood-brain barrier than P-gp, something that is difficult to assess with the currently available tools. This would make P-gp the dominant player, and, at least in the blood-brain barrier, only when P-gp is absent the contribution of Abcg2 becomes visible. As mentioned above, we have shown earlier that there is not a higher level of P-gp RNA in Abcg2 KO intestine. Although it therefore seems unlikely, we cannot completely exclude that there is increased expression of blood-brain barrier P-gp in Abcg2 KO mice. Be that as it may, it is clear that both P-gp and Abcg2 can contribute to decreased brain accumulation of dasatinib. The relevance of this finding may be put in perspective by the recent findings of Porkka et al. (30), who showed that dasatinib has antitumor activity in a mouse model of intracranial CML.

[3] Unpublished data.

Dasatinib also induced substantial responses in patients with CNS Ph+ leukemia and showed a considerably higher CNS accumulation than imatinib in mice and humans (30). Interestingly, imatinib failed to show any antitumor activity in their mouse model of intracranial CML, which is consistent with several clinical and preclinical findings (22, 28, 42, 43). This difference between dasatinib and imatinib cannot simply be explained by the fact that brain accumulation of imatinib is limited by P-gp and ABCG2 (21, 22, 27, 42, 43). In fact, our data show that P-gp and Abcg2 also profoundly restrict the brain accumulation of dasatinib in mice. Moreover, compared with other agents that have a good accumulation of the blood-brain barrier, such as cytarabine, the CNS accumulation of dasatinib is still low (44). Therefore, other factors, such as its far higher potency (325-fold) compared with imatinib (11), may explain the antitumor effects of dasatinib within the CNS.

We further showed that the brain accumulation of dasatinib in WT mice could be markedly increased with the dual P-gp and ABCG2 inhibitor elacridar. Moreover, WT mice pretreated with elacridar had similar dasatinib brain-to-plasma ratios as observed for *Abcb1a/1b;Abcg2*$^{-/-}$ mice that received either vehicle or elacridar. These results suggest that elacridar can fully inhibit P-gp and ABCG2 at the blood-brain barrier. We realize that results obtained in mice cannot simply be transferred to the clinical situation. However, we believe that our observations provide a rationale for combining dasatinib with a dual P-gp and ABCG2 inhibitor to increase the dasatinib brain accumulation and further improve its therapeutic efficacy in patients with CNS Ph+ leukemia. Clearly, further preclinical and clinical research is warranted to assess the feasibility of this approach.

Disclosure of Potential Conflicts of Interest

No potential conflicts of interest were disclosed.

Acknowledgments

We thank Evita van de Steeg and Marijn Vlaming for critical reading of the manuscript.

References

1. Borst P, Oude Elferink RP. Mammalian ABC transporters in health and disease. Annu Rev Biochem 2002;71:537–92.
2. O'Brien SG, Guilhot F, Larson RA, et al. Imatinib compared with interferon and low-dose cytarabine for newly diagnosed chronic-phase chronic myeloid leukemia. N Engl J Med 2003;348:994–1004.
3. Druker BJ, Sawyers CL, Kantarjian H, et al. Activity of a specific inhibitor of the BCR-ABL tyrosine kinase in the blast crisis of chronic myeloid leukemia and acute lymphoblastic leukemia with the Philadelphia chromosome. N Engl J Med 2001;344:1038–42.
4. Talpaz M, Silver RT, Druker BJ, et al. Imatinib induces durable hematologic and cytogenetic responses in patients with accelerated phase chronic myeloid leukemia: results of a phase 2 study. Blood 2002;99:1928–37.
5. Shannon KM. Resistance in the land of molecular cancer therapeutics. Cancer Cell 2002;2:99–102.
6. McCormick F. New-age drug meets resistance. Nature 2001;412:281–2.
7. Heinrich MC, Corless CL, Blanke CD, et al. Molecular correlates of imatinib resistance in gastrointestinal stromal tumors. J Clin Oncol 2006;24:4764–74.
8. Sleijfer S, Wiemer E, Seynaeve C, Verweij J. Improved insight into resistance mechanisms to imatinib in gastrointestinal stromal tumors: a basis for novel approaches and individualization of treatment. Oncologist 2007;12:719–26.
9. Gambacorti-Passerini C, Zucchetti M, Russo D, et al. α1 Acid glycoprotein binds to imatinib (STI571) and substantially alters its pharmacokinetics in chronic myeloid leukemia patients. Clin Cancer Res 2003;9:625–32.
10. Lombardo LJ, Lee FY, Chen P, et al. Discovery of *N*-(2-chloro-6-methyl-phenyl)-2-(6-(4-(2-hydroxyethyl)-piperazin-1-yl)-2-methylpyrimidin-4-ylamino)thiazole-5-carboxamide (BMS-354825), a dual Src/Abl kinase inhibitor with potent antitumor activity in preclinical assays. J Med Chem 2004;47:6658–61.
11. O'Hare T, Walters DK, Stoffregen EP, et al. *In vitro* activity of Bcr-Abl inhibitors AMN107 and BMS-354825 against clinically relevant imatinib-resistant Abl kinase domain mutants. Cancer Res 2005;65:4500–5.
12. Shah NP, Tran C, Lee FY, Chen P, Norris D, Sawyers CL. Overriding imatinib resistance with a novel ABL kinase inhibitor. Science 2004;305:399–401.
13. Hochhaus A, Kantarjian HM, Baccarani M, et al. Dasatinib induces notable hematologic and cytogenetic responses in chronic-phase chronic myeloid leukemia after failure of imatinib therapy. Blood 2007;109:2303–9.
14. Cortes J, Rousselot P, Kim DW, et al. Dasatinib induces complete hematologic and cytogenetic responses in patients with imatinib-resistant or -intolerant chronic myeloid leukemia in blast crisis. Blood 2007;109:3207–13.
15. Guilhot F, Apperley J, Kim DW, et al. Dasatinib induces significant hematologic and cytogenetic responses in patients with imatinib-resistant or -intolerant chronic myeloid leukemia in accelerated phase. Blood 2007;109:4143–50.
16. Kantarjian H, Pasquini R, Hamerschlak N, et al. Dasatinib or high-dose imatinib for chronic-phase chronic myeloid leukemia after failure of first-line imatinib: a randomized phase 2 trial. Blood 2007;109:5143–50.
17. Ottmann O, Dombret H, Martinelli G, et al. Dasatinib induces rapid hematologic and cytogenetic responses in adult patients with Philadelphia chromosome positive acute lymphoblastic leukemia with resistance or intolerance to imatinib: interim results of a phase 2 study. Blood 2007;110:2309–15.
18. Hamada A, Miyano H, Watanabe H, Saito H. Interaction of imatinib mesilate with human P-glycoprotein. J Pharmacol Exp Ther 2003;307:824–8.
19. Burger H, van Tol H, Boersma AW, et al. Imatinib mesylate (STI571) is a substrate for the breast cancer resistance protein (BCRP)/ABCG2 drug pump. Blood 2004;104:2940–2.
20. Houghton PJ, Germain GS, Harwood FC, et al. Imatinib mesylate is a potent inhibitor of the ABCG2 (BCRP) transporter and reverses resistance to topotecan and SN-38 *in vitro*. Cancer Res 2004;64:2333–7.
21. Breedveld P, Pluim D, Cipriani G, et al. The effect of Bcrp1 (Abcg2) on the *in vivo* pharmacokinetics and brain penetration of imatinib mesylate (Gleevec): implications for the use of breast cancer resistance protein and P-glycoprotein inhibitors to enable the brain penetration of imatinib in patients. Cancer Res 2005;65:2577–82.
22. Dai H, Marbach P, Lemaire M, Hayes M, Elmquist WF. Distribution of STI-571 to the brain is limited by P-glycoprotein-mediated efflux. J Pharmacol Exp Ther 2003;304:1085–92.
23. Bihorel S, Camenisch G, Lemaire M, Scherrmann JM. Influence of breast cancer resistance protein (Abcg2) and p-glycoprotein (Abcb1a) on the transport of imatinib mesylate (Gleevec) across the mouse blood-brain barrier. J Neurochem 2007;102:1749–57.
24. Bihorel S, Camenisch G, Lemaire M, Scherrmann JM. Modulation of the brain distribution of imatinib and its metabolites in mice by valspodar, zosuquidar and elacridar. Pharm Res 2007;24:1720–8.
25. Mahon FX, Belloc F, Lagarde V, et al. MDR1 gene overexpression confers resistance to imatinib mesylate in leukemia cell line models. Blood 2003;101:2368–73.
26. Nakanishi T, Shiozawa K, Hassel BA, Ross DD. Complex interaction of BCRP/ABCG2 and imatinib in BCR-ABL-expressing cells: BCRP-mediated resistance to imatinib is attenuated by imatinib-induced reduction of BCRP expression. Blood 2006;108:678–84.
27. Oostendorp RL, Buckle T, Beijnen JH, van Tellingen O, Schellens JH. The effect of P-gp (Mdr1a/1b), BCRP (Bcrp1) and P-gp/BCRP inhibitors on the *in vivo* absorption, distribution, metabolism and excretion of imatinib. Invest New Drugs 2009;27:31–40.
28. Pfeifer H, Wassmann B, Hofmann WK, et al. Risk and prognosis of central nervous system leukemia in patients with Philadelphia chromosome-positive acute leukemias treated with imatinib mesylate. Clin Cancer Res 2003;9:4674–81.
29. Leis JF, Stepan DE, Curtin PT, et al. Central nervous system failure in patients with chronic myelogenous leukemia lymphoid blast crisis and Philadelphia chromosome positive acute lymphoblastic leukemia treated with imatinib (STI-571). Leuk Lymphoma 2004;45:695–8.
30. Porkka K, Koskenvesa P, Lundan T, et al. Dasatinib crosses the blood-brain barrier and is an efficient therapy for central nervous system Philadelphia chromosome-positive leukemia. Blood 2008;112:1005–12.
31. Deguchi Y, Kimura S, Ashihara E, et al. Comparison of imatinib, dasatinib, nilotinib and INNO-406 in imatinib-resistant cell lines. Leuk Res 2008;32:980–3.
32. Hiwase DK, Saunders V, Hewett D, et al. Dasatinib cellular uptake and efflux in chronic myeloid leukemia cells: therapeutic implications. Clin Cancer Res 2008;14:3881–8.
33. Giannoudis A, Davies A, Lucas CM, Harris RJ, Pirmohamed M, Clark RE. Effective dasatinib uptake may occur without human organic cation transporter 1 (hOCT1): implications for the treatment of imatinib

resistant chronic myeloid leukaemia. Blood 2008;112:3348–54.

34. Evers R, Kool M, van Deemter L, et al. Drug export activity of the human canalicular multispecific organic anion transporter in polarized kidney MDCK cells expressing cMOAT (MRP2) cDNA. J Clin Invest 1998;101:1310–9.

35. Jonker JW, Buitelaar M, Wagenaar E, et al. The breast cancer resistance protein protects against a major chlorophyll-derived dietary phototoxin and protoporphyria. Proc Natl Acad Sci U S A 2002;99:15649–54.

36. Schinkel AH, Wagenaar E, van Deemter L, Mol CA, Borst P. Absence of the mdr1a P-glycoprotein in mice affects tissue distribution and pharmacokinetics of dexamethasone, digoxin, and cyclosporin A. J Clin Invest 1995;96:1698–705.

37. Huisman MT, Chhatta AA, van Tellingen O, Beijnen JH, Schinkel AH. MRP2 (ABCC2) transports taxanes and confers paclitaxel resistance and both processes are stimulated by probenecid. Int J Cancer 2005;116:824–9.

38. Schinkel AH, Mayer U, Wagenaar E, et al. Normal viability and altered pharmacokinetics in mice lacking mdr1-type (drug-transporting) P-glycoproteins. Proc Natl Acad Sci U S A 1997;94:4028–33.

39. Jonker JW, Freeman J, Bolscher E, et al. Contribution of the ABC transporters Bcrp1 and Mdr1a/1b to the side population phenotype in mammary gland and bone marrow of mice. Stem Cells 2005;23:1059–65.

40. Goh LB, Spears KJ, Yao D, et al. Endogenous drug transporters in *in vitro* and *in vivo* models for the prediction of drug disposition in man. Biochem Pharmacol 2002;64:1569–78.

41. Kamath AV, Wang J, Lee FY, Marathe PH. Preclinical pharmacokinetics and *in vitro* metabolism of dasatinib (BMS-354825): a potent oral multi-targeted kinase inhibitor against SRC and BCR-ABL. Cancer Chemother Pharmacol 2008;61:365–76.

42. Takayama N, Sato N, O'Brien SG, Ikeda Y, Okamoto S. Imatinib mesylate has limited activity against the central nervous system involvement of Philadelphia chromosome-positive acute lymphoblastic leukaemia due to poor penetration into cerebrospinal fluid. Br J Haematol 2002;119:106–8.

43. Bornhauser M, Jenke A, Freiberg-Richter J, et al. CNS blast crisis of chronic myelogenous leukemia in a patient with a major cytogenetic response in bone marrow associated with low levels of imatinib mesylate and its *N*-desmethylated metabolite in cerebral spinal fluid. Ann Hematol 2004;83:401–2.

44. Slevin ML, Piall EM, Aherne GW, Johnston A, Lister TA. The pharmacokinetics of cytosine arabinoside in the plasma and cerebrospinal fluid during conventional and high-dose therapy. Med Pediatr Oncol 1982;10 Suppl 1:157–68.

Clinical Cancer Research

Brain Accumulation of Dasatinib Is Restricted by P-Glycoprotein (ABCB1) and Breast Cancer Resistance Protein (ABCG2) and Can Be Enhanced by Elacridar Treatment

Jurjen S. Lagas, Robert A.B. van Waterschoot, Vicky A.C.J. van Tilburg, et al.

Clin Cancer Res 2009;15:2344-2351.